IOPscience iopscience.iop.org

Home Search Collections Journals About Contact us My IOPscience

Searching for the proper law of dislocation multiplication in covalent crystals

This article has been downloaded from IOPscience. Please scroll down to see the full text article.

2002 J. Phys.: Condens. Matter 14 12887

(http://iopscience.iop.org/0953-8984/14/48/329)

View the table of contents for this issue, or go to the journal homepage for more

Download details:
IP Address: 171.66.16.97
The article was downloaded on 18/05/2010 at 19:13

Please note that terms and conditions apply.

INSTITUTE OF PHYSICS PUBLISHING JOURNAL OF PHYSICS: CONDENSED MATTER

J. Phys.: Condens. Matter **14** (2002) 12887–12895 PII: S0953-8984(02)54014-5

Searching for the proper law of dislocation multiplication in covalent crystals

Jan Fikar[1], **Bernard Viguier**[2], **Tomas Kruml**[1] **and Corinne Dupas**[1]

[1] IPMC, FSB, Ecole Polytechnique Fédérale de Lausanne, CH 1015 Lausanne, Switzerland
[2] CIRIMAT, Ecole Nationale Supérieure des Ingénieurs en Arts Chimiques et Technologiques, Toulouse, France

E-mail: Tomas.Kruml@epfl.ch

Received 27 September 2002
Published 22 November 2002
Online at stacks.iop.org/JPhysCM/14/12887

Abstract

A simple model based on dislocation theory allows the construction of a fully defined system of differential equations and the calculation of curves that correspond to different mechanical tests such as stress relaxation, the creep test and the imposed strain rate test. Various multiplication and exhaustion rates of mobile dislocations have been considered. The numerical solution of the system reproduces satisfactorily experimental curves obtained in Ge single crystals at 750 K.

1. Introduction

In the 1960s Alexander and Haasen [1] published a model describing quantitatively the plastic behaviour of covalent crystals with the diamond lattice (the A&H model). As had already been recognized by these authors, one of the key issues of the problem is to predict the evolution with strain and stress of the mobile dislocation density ρ_m. The model that they proposed contains in particular a relation for dislocation multiplication, which can be expressed in terms of the time derivative of the density

$$\dot{\rho}_{multi} = K_{multi1}\dot{\gamma}_p\tau_{eff}, \tag{1}$$

where $\dot{\gamma}_p$ is the plastic strain rate, τ_{eff} is the effective stress and K is a constant. This relation is derived from the results of etch pit experiments. Contrary to the usual law for dislocation multiplication which is assumed in metals, and for which the multiplication rate is simply proportional to the area swept by dislocations

$$\dot{\rho}_{multi} = K_{multi2}\dot{\gamma}_p, \tag{2}$$

relation (1) contains the effective stress. Nevertheless, τ_{eff} is implicitly taken into account in (2), where it influences the plastic strain rate through the dislocation velocity. Therefore, its meaning in relation (1), where it is explicitly added, is not clear from the theoretical point of

 © 2002 IOP Publishing Ltd Printed in the UK

view. However, the A&H model has been very successful in reproducing the characteristics of the yield point at the onset of the deformation curve, including its temperature and strain-rate dependence. This has been considered as a proof for the validity of relation (1). It has been discovered only recently that the successful predictions of the A&H model concerning the lower yield point (LYP) do not in fact depend on the actual multiplication law [2]. This finding reopens the question of which is the appropriate multiplication law in semiconductors.

In the same study, Moulin *et al* [2] performed three-dimensional mesoscopic simulations of dislocation dynamics in silicon. In this way they reproduced numerically the yielding in the stress–strain curve and they proposed a different dislocation multiplication law that fits the results of the simulation as well as the previous experimental results

$$\dot{\rho}_{multi} = K_{multi3}\dot{\gamma}_p\sqrt{\tau_{eff}/\rho_m}. \tag{3}$$

The aim of this paper is to present a calculation procedure that allows us to test the proposed relations (1)–(3). The calculated curves are compared with experimental results concerning the plasticity of Ge single crystals that have been obtained in our laboratory in terms of stress–strain curves and transient tests (stress relaxation and creep tests) [3].

2. Constitutive equations

The main idea of the presented calculation is to relate microscopic features, such as the behaviour of the whole dislocation population (density, velocity and their dependence on strain and stress), to the macroscopic variable that can be experimentally measured (applied stress and macroscopic strain). We may also take advantage of the calculation to determine parameters which are very difficult to measure experimentally, such as the ratio of mobile to total dislocation densities or the internal stress. From a macroscopic point of view, the straining experiment is depicted by the so-called machine equation, which may take a different formulation depending on the kind of test involved. This equation is described later.

The Orowan law relates plastic strain rate $\dot{\gamma}_p$ to mobile dislocation density ρ_m and velocity v ($b = 4.0 \times 10^{-10}$ m is the Burgers vector)

$$\dot{\gamma}_p = bv\rho_m. \tag{4}$$

Whereas a number of observations report values for the dislocation density, it is impossible to determine experimentally which part of this population is mobile, i.e. participates in the plastic deformation at a given time. Therefore we have to distinguish between mobile and total dislocation densities as detailed later. Under some conditions the dislocation velocity can be measured, and those values will be used as an input in the calculation. This allows us to reduce the number of fitted parameters.

2.1. Dislocation velocity

The velocity of screw dislocations has been measured using double etch pit experiments at different temperatures and for stresses ranging from 10 to 50 MPa [3]. The obtained velocities depend on stress according to the power law

$$v = v_0(\tau_{eff}/\mu)^m. \tag{5}$$

Such a law is no doubt a very simplified description of reality. It assumes implicitly the homogeneous deformation of the specimen, which is likely not to be the case for semiconductors [3]. Further, the screws are less mobile than the 60° dislocations, so the parameters of law (5), measured for screws, underestimate the 'average' dislocation velocity. For covalent compounds, the velocity of dislocations shorter than roughly 5 μm (see [4])

depends on their length and is less than the velocity in the length-independent regime, depicted by the power law (5). At low stresses, dislocations may be slowed down by interaction with impurities. Coefficient m, regarded as a constant, is in fact slightly stress dependent [5]. However, the latter two effects were not observed in etch pit experiments. Furthermore, the calculations are limited to a fixed temperature $T = 750$ K for which the parameters of the power law (5) were measured as $v_0 = 16 \pm 5$ m s^{-1} and $m = 2.1 \pm 0.2$.

The effective stress τ_{eff} is the difference between the applied stress τ and the internal stress τ_i, given by the Taylor formula

$$\tau_{eff} = \tau - \tau_i = \tau - \alpha\mu b\sqrt{\rho_t}, \tag{6}$$

where $\mu = 56$ GPa is the shear modulus and α is a dimensionless parameter characterizing the dislocation interaction. α could be fitted in the model; nevertheless it is more advantageous to limit the number of free parameters as much as possible, therefore $\alpha = 1/\pi$ is introduced, as measured by Berner and Alexander [6]. ρ_t is the density of dislocations which are responsible for work-hardening. It is assumed that ρ_t equals the total dislocation density.

2.2. Dislocation density

A distinction has been made between the density of mobile dislocations ρ_m and the total dislocation density ρ_t which also includes the dislocations locked in the crystal. During plastic straining, both populations may evolve. In order to model this evolution, the following processes have been included in the calculations:

(i) the multiplication of mobile dislocations $\dot{\rho}_{multi}$
(ii) the escape of dislocations at the free surfaces $\dot{\rho}_{surf}$ and
(iii) the locking of mobile dislocations within the crystal $\dot{\rho}_{ex}$.

Note that the decrease in dislocation density through mutual annihilation of dislocations within the crystal has been neglected. This mechanism is supposed to be important at high strain levels, but we limit our calculation to moderate plastic strains (25% resolved).

The multiplication of dislocations increases the number of both mobile and total dislocations. Three formulations (1)–(3) have already been introduced for the multiplication. The loss of mobile dislocations at the free specimen surface is

$$\dot{\rho}_{surf} = -\frac{2}{b\ell}\dot{\gamma}_p, \tag{7}$$

where ℓ is the dimension of the crystal in the slip direction.

The locking of mobile dislocations corresponds to the exhaustion of mobile dislocations. It decreases the density of mobile dislocations and does not affect the total dislocation density. An example of such a process is dipole formation which was frequently detected in TEM observations [3]. Three laws (8)–(10) for the exhaustion of mobile dislocations were tested

$$\dot{\rho}_{ex} = K_{ex1}\dot{\gamma}_p, \tag{8}$$

$$\dot{\rho}_{ex} = K_{ex2}\dot{\gamma}_p\rho_t, \tag{9}$$

$$\dot{\rho}_{ex} = K_{ex3}\dot{\gamma}_p\sqrt{\rho_t}. \tag{10}$$

The evolution of the density of both sets of dislocations may be written as

$$\dot{\rho}_m = \dot{\rho}_{multi} - \dot{\rho}_{ex} - \dot{\rho}_{surf}, \tag{11}$$

for the density of mobile dislocations and

$$\dot{\rho}_t = \dot{\rho}_{multi} - \dot{\rho}_{surf}, \tag{12}$$

for the total dislocation density.

2.3. Relation to experiments

During any deformation experiment, the applied strain rate $\dot{\gamma}_a$ is related to the specimen plastic strain $\dot{\gamma}_p$ and to the applied stress rate $\dot{\tau}$ through the so-called 'machine equation'

$$\dot{\tau} = M(\dot{\gamma}_a - \dot{\gamma}_p), \tag{13}$$

where M is the elastic modulus of the straining apparatus and specimen assembly. The total strain rate $\dot{\gamma}$ can be decomposed into plastic and elastic parts

$$\dot{\gamma} = \dot{\gamma}_p + \frac{\dot{\tau}}{E}, \tag{14}$$

where E is the slope of the elastic part of the stress–strain curve and τ and γ are the measured resolved stress and resolved strain.

When the Orowan law (4) and the definition of the effective stress (6) are introduced in equations (13) and (14), the experimental values (τ, γ) are directly related to the evolution of the dislocation densities (ρ_m, ρ_t). The fully determined system of four differential equations (11)–(14) for four variables $(\tau, \gamma, \rho_m, \rho_t)$ is now defined. Relations (11) and (12) contain one multiplication law (1)–(3) together with one exhaustion law (8)–(10); thus there exist nine different systems to solve.

To calculate the stress–strain curve, the applied strain rate is fixed to the experimental value. For the creep transient, the system is reduced to three equations and three variables since τ is constant and equations (13) and (14) can be written $\dot{\gamma} = \dot{\gamma}_p (= \dot{\gamma}_a)$. For the stress relaxation experiment, the crosshead is stopped ($\dot{\gamma}_a = 0$) and equations (13) and (14) are reduced to $\dot{\tau} = -M\dot{\gamma}_p$.

2.4. Fitting procedure

The systems of differential equations (11)–(14) are integrated numerically. All the parameters are either known from the previous experiments or fixed by the experimental conditions, except for the parameters K_{multi_I} and K_{ex_J} where I and J refer to the particular multiplication and exhaustion laws used. For stress relaxation, creep and imposed strain rate tests, the experimental curves were independently calculated and the coefficients K_{multi_I} and K_{ex_J} fitted in order to minimize the quadratic difference Ω between experimental and calculated curves by the Nelder–Mead simplex method. The function Ω was chosen in the form

$$\Omega = \frac{1}{(\tau_{\max} - \tau_{\min})^2} \sum_{i=1}^{N} \Delta\tau_i^2 + \frac{1}{(\gamma_{\max} - \gamma_{\min})^2} \sum_{i=1}^{N} \Delta\gamma_i^2, \tag{15}$$

in order to give the relative deviations in τ and γ the same weight; $\Delta\tau_i$ and $\Delta\gamma_i$ are differences between measured and calculated stress and strains, N is the total number of data and $\tau_{\max}$, $\tau_{\min}$, $\gamma_{\max}$ and $\gamma_{\min}$ are extremal values in the data set.

The initial conditions were obtained differently for the transient experiments and the stress–strain curve. In the case of transient experiments, the initial stress and strain level are fixed by the experimental conditions. The initial values of ρ_m and ρ_t were adjusted in such a way that $\dot{\gamma}_p$ at the onset of the transient is correctly fitted. For the stress–strain curve, the integration starts at the upper yield point (UYP) where $\dot{\tau} = 0$ and $\dot{\gamma}_p$ is therefore given by the machine-imposed strain rate. Initial ρ_m and ρ_t values were calculated from (4) assuming that at this point all dislocations are mobile. Next, the fit of coefficients K_{multi_I} and K_{ex_J} is performed on the part of the stress–strain curve after the UYP. The deduced values are then used to reproduce the beginning of the curve (before the UYP).

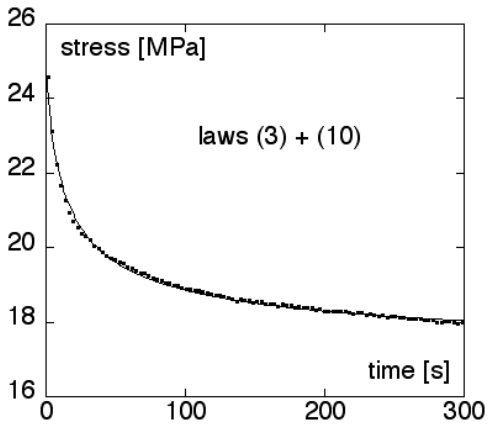

Figure 1. Comparison between experimental (dots) and calculated (thin curve) results for a stress relaxation experiment performed after the LYP.

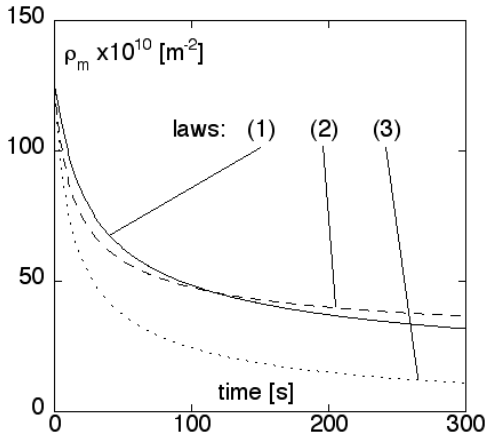

Figure 2. Evolution of the mobile dislocation density during the stress relaxation in figure 1 according to calculations performed using the exhaustion law (10) and the three multiplication laws.

3. Mechanical tests

Single-crystalline paralellepipedic specimens of dimensions $4 \times 4 \times 9$ mm^3 were compressed in a Schenck RMC 100 machine at 750 K under an He atmosphere. The single slip $[\bar{1}23]$ orientation of the specimen axis was chosen. Constant strain rate tests ($\dot{\gamma}_a = 1.1 \times 10^{-4}$ s^{-1}) as well as short transient tests were conducted at various strain levels, both before and after the UYP. More details about the experimental set-up and procedure used can be found in [7].

4. Results and discussion

The comparison of calculated and experimental curves was started by examining the transient experiments because the system of differential equations is simpler in this case.

Figure 1 presents the experimental data for a stress relaxation together with the calculated curve for the combination of the multiplication law (3) and the exhaustion law (10).

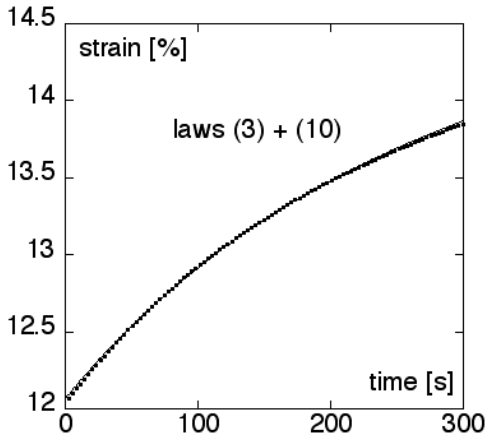

Figure 3. Comparison between experimental (dots) and calculated (thin curve) results for a creep experiment performed after the LYP.

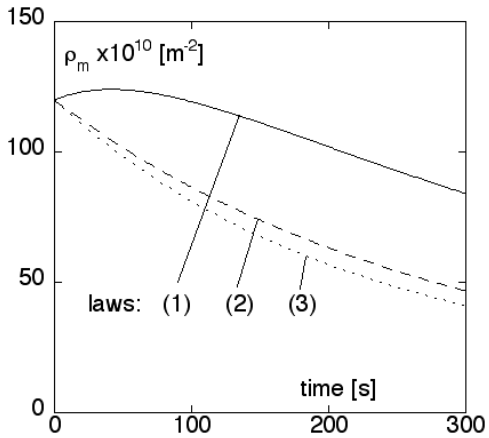

Figure 4. Evolution of the mobile dislocation density during the creep test of figure 3 according to calculations performed using the exhaustion law (10) and the three multiplication laws.

The agreement between measured and calculated curves is excellent. An analogous comparison is done for all nine combination of three multiplication and three exhaustion laws. The evolution of the mobile dislocation density during this stress relaxation for the three multiplication laws is shown in figure 2, and once again these three laws give very similar results.

The same comparison between experimental and calculated curves is presented in figure 3 for a creep transient performed at 12% total strain. Very good agreement between the curves is found for each multiplication and exhaustion combination used. The evolution of the density of mobile dislocations is shown in figure 4 as calculated for the exhaustion law (10) and the three multiplication laws. Figure 4 shows that the difference between the various laws does not imply a very different behaviour of the dislocation population, despite the less rapid variation of ρ_m when using the law (1).

Apart from the two examples of transient test calculation shown above, other comparisons were made. In particular we successfully reproduced relaxation and creep tests with a very

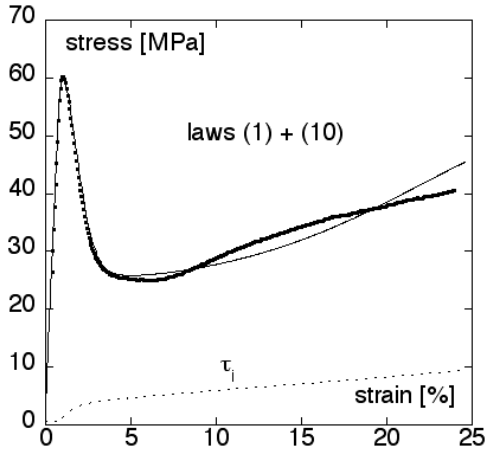

Figure 5. The whole experimental stress–strain curve (dots) of Ge at 750 K is compared with the calculated curve (thin continuous curve) for multiplication law (1) and exhaustion law (10). The calculated internal stress is shown (dotted curve).

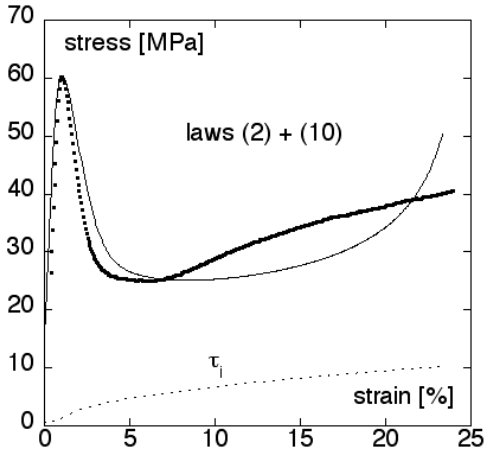

Figure 6. Same as figure 5 but the calculations are performed using multiplication law (2) and exhaustion law (10).

uncommon shape before the upper yield stress [7]. It was not possible to determine which of the proposed equations for multiplication and exhaustion of dislocation could be disregarded, since we could fit the experimental curves well with any combination. Nevertheless, the proposed model reproduces very well the measured curves in spite of having only two fitted parameters. Furthermore, many features are observed as output of the calculations which are in full agreement with the measurements of dislocation densities and internal stresses and with our current understanding of dislocation behaviour along the stress–strain curve. The observations apply to the transient experiments:

- before the LYP, almost no exhaustion is observed during transients;
- after the LYP, multiplication is small compared with exhaustion;
- ρ_m is found to be of the order of 10^9 m^{-2} before the UYP and 10^{12} after the LYP;
- the internal stress is negligible before the UYP but not after the LYP.

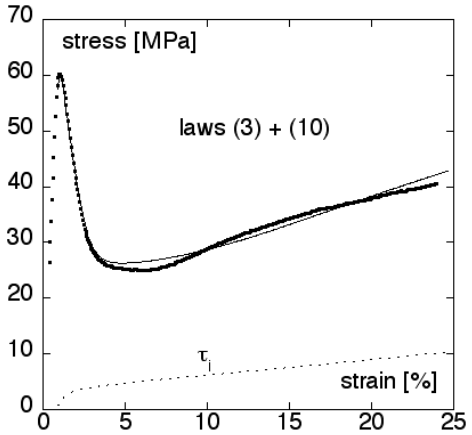

Figure 7. Same as figure 5, but the calculations are performed using multiplication law (3) and exhaustion law (10).

The fact that it is not possible to classify the laws for the evolution of dislocation densities may be related to the transient character of the above experiment. Indeed, stress and strain variations are quite small during such tests. For this reason, the study has been complemented by extending the comparison to the whole stress–strain curve.

Whole stress–strain curves are shown in figures 5–7, where experimental points and curves calculated using the exhaustion law (10) and multiplication laws (1)–(3) are superimposed. The results for each of the three exhaustion laws (8)–(10) are not shown here since they do not have much effect on the results, i.e. the relative behaviour of the different multiplication laws deduced using law (10) is still valid for the other two exhaustion laws. Examination of the stress–strain curves in figures 5–7 reveals first that the yielding behaviour is correctly reproduced by any combination of laws. Some differences appear between the multiplication laws when observing the whole curve. Figure 6 indicates that the classic multiplication law (2) used for metals does not allow us to correctly reproduce the part of the curve at high strain, since the stress diverges at the end of the deformation. The comparison between figures 5 and 7 suggests that equations (1) and (3) are both able to reproduce satisfactorily the experimental curves. However, the agreement is not perfect for either of the two laws. The strain hardening rate seems to be too high for relation (1). When reproducing the stress–strain curve from the UYP to the beginning with relation (3), the dislocation density decreases too fast and reaches zero at the point where the calculated curve in figure 7 starts. In order to test further the ability of such equations to reproduce the experimental curves, it is apparently necessary to extend the present comparison for different straining temperatures. This necessitates, in the present formalism, experimental measurement of the dislocation velocities in the correct stress range for various temperatures. That work is in progress in our laboratory.

Besides testing the existing models, the present calculations also allow us to follow the evolution of normally hidden parameters, such as the internal stress (equivalent to the square root of the total dislocation density) and the density of mobile dislocations. For all the combinations tested it is observed that the internal stress increases along the curve as ρ_t increases. The density of mobile dislocations, shown in figure 8, increases sharply from the beginning, passes through a maximum and then decreases. The maximum rate of increase in ρ_m corresponds to the UYP while it is interesting to note that the maximum of the density occurs at a strain level lower (by about 1%) than the LYP for the laws (1) and (3) (see figure 8).

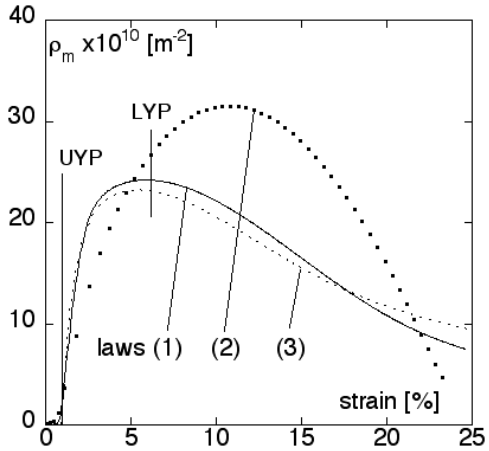

Figure 8. Evolution of the mobile dislocation density during the stress–strain curve of figures 5–7 according to calculations performed using the exhaustion law (10) and the three multiplication laws. The positions of the UYP and the LYP are marked.

5. Conclusions

A calculation procedure with only two fitting parameters has been developed. This procedure allows us to reproduce stress relaxations and creep tests as well as the whole stress–strain curve for single-crystalline Ge at 750 K. It is shown that the multiplication law usually used for metals (equation (2)) does not allow us to reproduce the experimental results. At the present stage, it is not possible to discriminate between the multiplication laws proposed by Alexander and Haasen (equation (1)) and the recent proposition by Moulin *et al* (equation (3)). The calculation of stress–strain curves at different temperatures seems to be necessary to further clarify the multiplication process in semiconductors.

References

[1] Alexander H and Haasen P 1968 *Solid. State Phys.* **22** 27
[2] Moulin A, Condat M and Kubin L 1999 *Acta Mater.* **47** 2879
[3] Dupas C, Zuodar N, Coddet O, Kruml T and Martin J L 2002 *J. Phys.: Condens. Matter* **14** 12989
[4] Kruml T, Caillard D, Dupas C and Martin J L 2002 *J. Phys.: Condens. Matter* **14** 12897
[5] Caillard D and Martin J L 2003 *Dislocation Based Mechanisms of Crystal Plasticity* (Amsterdam: Elsevier) at press
[6] Berner K and Alexander H 1967 *Acta Metall.* **15** 933
[7] Charbonnier C, Kruml T and Martin J L 2001 *Multiscale Modelling of Materials (MRS Symp. Proc. vol 653c)* (Warrendale, PA: Materials Research Society) p Z5.7.1